Materials Science Forum
ISSN: 1662-9752, Vol. 1183, pp 55-67
doi:10.4028/p-y3MapP

Submitted: 2026-01-19
Revised: 2026-02-16
Accepted: 2026-02-24
Online: 2026-04-13

Fast Inverse Identification of the Coefficient of Friction in Cold Strip Rolling Using a Physics-Informed Neural Network

Christian Overhagen[1,a*] and Robert Martin[,2,b]

[1]University of Duisburg-Essen, Sustainable Metallurgy, Friedrich-Ebert-Strasse 12, 47119 Duisburg, Germany

[2]University of Duisburg-Essen, Mathematics for Engineers, Friedrich-Ebert-Strasse 12, 47119 Duisburg, Germany

[a]christian.overhagen@uni-due.de, [b]robert.martin@uni-due.de

Keywords: Cold Strip Rolling, Friction in Rolling, Inverse Parameter Identification, Physics-Informed Neural Network

Abstract. Friction plays an important role in flat rolling processes for the force and power demands, kinematics and final product quality. In search for a method of in-situ characterization of the coefficient of friction (COF) denoted by μ by non-contacting measurements, a method for determination of the COF from high-accuracy forward slip measurements, i.e. by laser doppler velocimetry combined with a comprehensive evaluation without simplifications is the method of choice. The evaluation must comprise the volume flux equilibrium at the neutral point and the roll gap exit, as well as the connection of the neutral point and COF by von Karman's ODE. This iterative procedure involves multiple solutions of the ODE as well as the nonlinear volume flux relation. In the present work, this problem is addressed by a physics-informed neural network (PINN), providing a rapid connection between the forward slip and the COF based on the mathematical rolling theory. The contribution shows that we can solve von Karman's ODE inversely by a PINN, enablind detection of the COF and the neutral angle from the measured forward slip.

Introduction

Friction is an important process parameter in hot and cold rolling, as it determines the force, work and power demands of the process and is of crucial meaning for the neutral point, connecting stress and velocity distributions in the roll gap. Hence, a fast non-contacting method for in-situ characterization of the friction coefficient in rolling is of great interest for process control, especially for interstand tension control in continuous multi-stand rolling mills.

State of the Art

The importance of the friction on the stress distribution and forward slip was already described by von Karman as well as Dresden in 1925 [19, 2]. Experimental methods of friction characterization can be subdivided in two groups: firstly, methods which attempt to measure the stress distribution in the roll gap directly by mechanical transducers. Secondly, indirect methods which leverage the measurement of process quantities which are influenced by friction, as forward slip. In the first group, Siebel and Lueg carried out rolling experiments using a pin-transducer embedded on the roll surface and were able to measure the stress distribution in the roll gap [15]. Similar experiments were reported by Sylwestrowicz, as well as van Rooyen and Backofen [16, 17] for hot and cold rolling. In 2006, experiments with a newly developed transducer were carried out by Arentoft et al and measured stress distributions were presented [5]. All of these methods have in common that the experimental transducers alter the rolling process in a way that such measurement devices cannot be introduced in a continuous practical rolling process, accompanying everyday industrial production.

A number of works discussed the friction measurement by forward slip, where a summary is given by Lenard, who came to the conclusion that the assessment of friction from forward slip was unreliable when simple formulae are used to relate these quantities [6]. However, Lundberg reports successful friction measurements in hot rolling, estimating the forward slip from billet head interstand times [8]. The fundamentals of the evaluation were laid out by Jarl, who pointed out the difficulties of this method and also used very simplistic relations [4]. For more precise measurement of the forward slip, laser-doppler velocimetry experiments were carried out by Li et al. with an uncertainty analysis [7].

Modeling of the flat rolling process. In flat rolling, a rectangular cross section with the initial height h_0 passes through two rotating tools with radius R, while its height is reduced to the exit height h_1. The geometry of the roll gap is shown in Figure 1. For the mathematical modeling of the stress distribution in this process, different methods are available. Nowadays, the Finite Element Method (FEM) has become a general-purpose tool for numerical analysis of metal forming processes. However, the process of cold strip rolling as treated in the present analysis has the geometrical nature that much more efficient modeling tools may used, for instance the classical slab method. As already shown by Pawelski, the results of stationary FEM calculations and the slab method are nearly identical for cold strip rolling [12]. Also, rolling models based on the slab method achieve high fidelity in comparison to measured values of roll force and torquein cold strip rolling, as already shown by Hessenberg and Sims [3]. Due to these reasons, FEM calculations are omitted in the current analysis and attention is paid to time-efficient simulations based on the slab method.

In 1925, Theodore von Karman published his contribution to the theory of the rolling process, in which an ordinary differential equation (ODE) was formulated on the basis of a differential force equilibrium on a strip element in the roll gap. Von Karman's ODE describes the gradient of the specific horizontal force $\sigma_x h$ (specific: per unit strip width) with respect to the x coordinate as a function of the normal and shear stresses,

$$\frac{d(\sigma_x h)}{dx} = 2\left(\sigma_N \pm \tau_F \tan\alpha\right). \tag{1}$$

The local roll gap inclination angle α is described by the spatial derivative of the strip thickness distribution,

$$\tan\alpha = \frac{1}{2}\frac{dh}{dx}. \tag{2}$$

The strip height distribution is given by the circular shape of the arc of contact,

$$h(x) = h_1 + 2R\left(1 - \sqrt{1 - \frac{x^2}{R^2}}\right). \tag{3}$$

For smaller contact angles, as in cold strip rolling, we may substitute the circular arc with the parabolic function

$$h(x) \approx h_1 + \frac{x^2}{R} \tag{4}$$

with the derivative

$$\frac{dh}{dx} = \frac{2x}{R}. \tag{5}$$

For the frictional shear stress τ_F, classical works of the rolling theory assume slipping friction with

$$\tau_F = \mu\sigma_N \tag{6}$$

or shearing friction according to

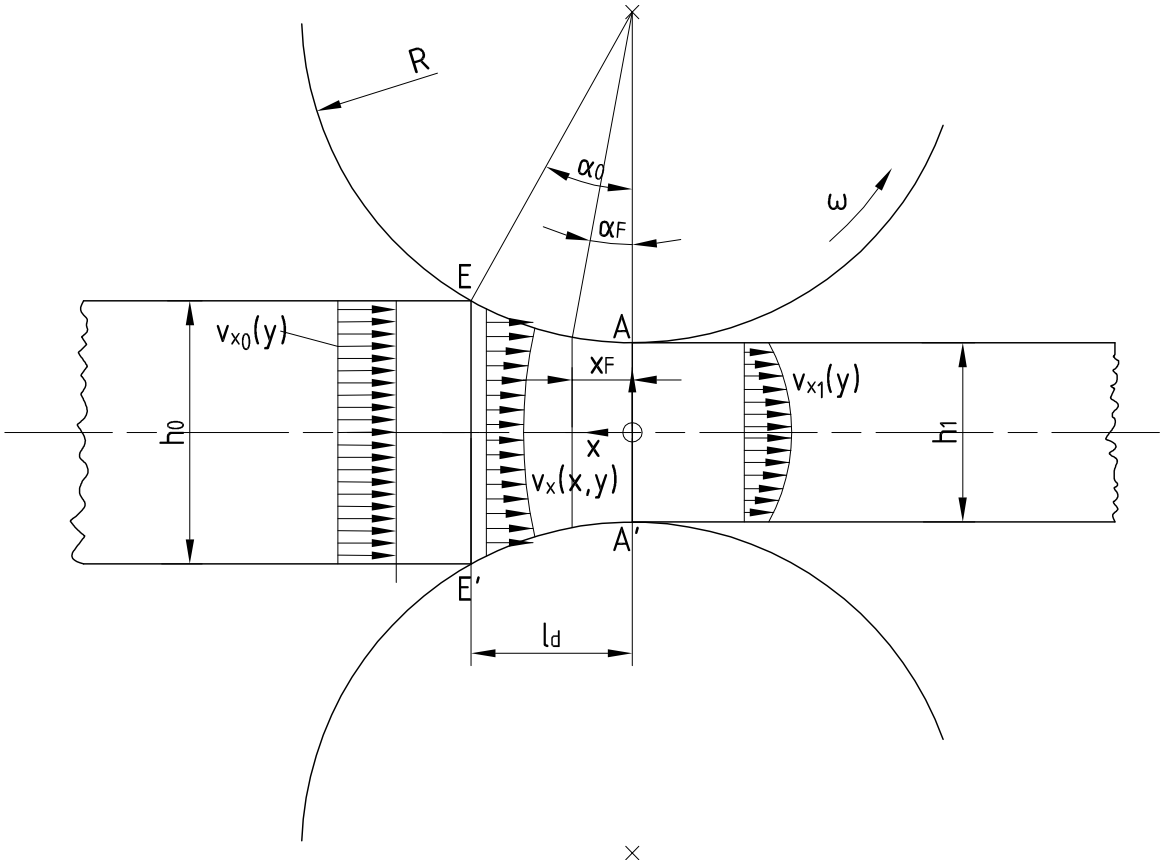

Fig. 1: Geometry of the roll gap. x_F: neutral point position

$$\tau_F = mk = m\frac{k_f}{\sqrt{3}}. \tag{7}$$

After simplified analytical solutions to von Karman's ODE were published by several authors, Alexander presented a numerical solution to the ODE by Runge-Kutte methods [1]. This solution was later extended by Venter and Abd-Rabbo [18] to include Orowan's theory of inhomogeneous deformation in rolling [9]. Their final ODEs are generally of the form

$$\frac{d\sigma_N}{d\alpha} = F(\sigma_N, \alpha) \text{ for slipping friction, and} \tag{8}$$

$$\frac{d\sigma_N}{d\alpha} = G(\alpha) \text{ for sticking friction.} \tag{9}$$

These can be solved numerically for the normal stress distributions $\sigma_N(\alpha)$. To construct an inverse method for determination of μ from a known neutral angle α_N, the whole process of numerical solution of the differential equations must be iterated several times, until a good approximation of μ is found, which satisfies the given α_N, increasing evaluation times substantially. If elastic roll flattening is accounted for, even an additional iteration loop enters the evaluation procedure, making the model difficult to use for online process applications.

Kinematical relationship of neutral point and forward slip. The solution of the ODE of the roll gap provides the distribution of the normal stress along the roll gap coordinate x or α. On the kinematics side, the basis is the constancy of the volume flux

$$\dot{V} = const = A_0 v_0 = A_1 v_1 = A(\alpha) v(\alpha), \tag{10}$$

expressing that the product of the cross section and the longitudinal velocity (in the direction normal to the cross sectional surface) is a constant value at any roll gap coordinate. Therefore, we can also apply this equation to the neutral plane at $\alpha = \alpha_N$, giving

$$A_1 v_1 = A_N v_N = A_N v_C \cos \alpha_N. \tag{11}$$

Here, A_N is the cross section in the neutral plane, v_C is the circumferential velocity of the roll and α_N the neutral angle. We may express the circumferential velocity by the angular roll velocity and the roll radius as $v_C = \omega R$, giving

$$\cos \alpha_N = \frac{A_1}{A_N} \frac{v_1}{\omega R}. \tag{12}$$

The forward slip κ relates the strip exit velocity to the circumferential roll velocity according to

$$\kappa = \frac{v_1 - v_c}{v_c} = \frac{v_1}{v_c} - 1 = \frac{v_1}{\omega R} - 1, \tag{13}$$

which allows us to express the neutral angle as

$$\cos \alpha_N = \frac{A_1}{A_N} (1 + \kappa). \tag{14}$$

We should note at this stage, that the absolute value of α_N (in radians) is strongly connected to the geometrical bite angle α_0, as $\alpha_N \in [0; \alpha_N]$. Therefore, we may define the dimensionless neutral angle β_N as

$$\beta_N = \frac{\alpha_N}{\alpha_0} \tag{15}$$

The cross sections A_1 (at exit) and A_N (at the neutral angle) can be described as the product of height and width at the respective positions,

$$A_1 = h_1 w_1, \tag{16}$$

and

$$A_N = h_M w_N. \tag{17}$$

When we disregard lateral spread, $w_0 = w_1 = w_N$, we can write

$$\frac{A_1}{A_N} = \frac{h_1}{h_N} \tag{18}$$

and therefore

$$\cos \alpha_N = \frac{h_1}{h_N} (1 + \kappa) = \frac{h_1 (1 + \kappa)}{h_1 + 2R (1 - \cos \alpha_N)}. \tag{19}$$

An analytical solution to this transcendental equation will be given later in this paper.

Physics-informed neural networks. Neural networks provide a framework for a wide range of modeling tasks. A set of input information features is passed through a number of hidden layers until it reaches the output layer. The passing through one layer is basically a vector-matrix multiplication followed by addition of a bias vector of the respective layer and application of an activation function to the results, which in turn are fed as inputs into the next layer. The manipulation of the data in each layer is influenced by the bias vectors and weight matrices, which constitute the model parameters. In order to evaluate the network successfully, the model parameters must be adjusted so that the network generates the intended outputs from the given inputs, according to the modeling task at hand. This adjustment procedure is called the training process. During the training, a loss function is evaluated

which assesses the quality of the prediction, based on which the network parameters are updated by an optimizer routine. This process is repeated many times (called the epochs) until the loss of the validation data (a subset of the total data, which is not used to update the model parameters) has reached a desirably low value. In each epoch, the training data is fed into the network in multiple batches. The batch size is the number of training samples processed in one forward and backward pass before the model's internal parameters (weights and biases) are updated [11].
The default method of training a neural network utilizes given input and target output data for the respective inputs. Typical default loss functions are based upon mean squared error losses, comparing the predicted outputs to the target outputs. A physics-informed neural network is a special form of training where the loss function is replaced by a special function which contains information about the physical nature of the problem to be solved, often in the form of (partial) differential equations. To handle differential equations, the loss function makes use of automatic differentiation provided by the machine learning framework used to check the gradients of the predicted outputs against a given differential equation. This opens a wide range of applications to the PINNs (physics informed neural networks), from the data-driven solution of differential equations, combined with data modeling, up to inverse parameter identification of physical models which are based on differential equations [13, 14]. PINNs are already used to solve metal forming problems, like roll pass design [10].

Aims of the Present Analysis

In the present paper, we will construct a physics-informed neural network to solve von Karman's ordinary differential equation of the roll gap. Two versions of the neural network will be presented, with the first being a forward model for predicting the stress distribution in the roll gap from the given friction coefficient. The purpose of the second model (the inverse model) is to accomplish an inverse parameter identification of the friction coefficient and find a physical friction coefficient μ which corresponds to a prescribed neutral angle. The kinematic relationship between the forward slip and neutral point position will be calculated analytically.

Scientific Methodology

In this section, we will present the models which were built to address the present problem of friction coefficient estimation from measured forward slip, while the results obtained will be presented in the next section.

Methods and tools. To tackle the present problem of the friction coefficient estimation from measured forward slip, a physics-informed neural network was trained using the PyTorch Machine Learning Framework [11] and Python programming language. Especially, PyTorch's automatic differentiation engine is leveraged to find the gradients of the predicted stress values in the form of a PINN as described by Raissi et al. [13]. The PINN solves von Karman's differential equation, and the friction coefficient μ is estimated from alignment of the solution with a normalized neutral angle β_N previously calculated from the measured forward slip. In the current state of development, the solution does not take elastic roll flattening into account. As this effect, prevalent in cold strip rolling, affects the length of the contact region and stress distribution, an impact on the results is to be expected. Therefore, we present numerical results accounting for roll flattening in the results section, obtained by classical numerical solution of von Karman's differential equation and Hitchcock's roll flattening model. Another simplification used in the analysis is that the friction coefficient is kept constant in the roll gap, which is owed to the fact that the forward slip measurement only provides a very global means of friction assessment, from which the way in which the friction coefficient changes throughout the roll gap cannot be deduced.
The actual industrial problem of cold rolling is therefore reduced to a mathematical inverse parameter identification problem for von Karman's differential equation, solved by a physics-informed neural network.

Forward solution of von Karman's ODE for rolling using a neural network.

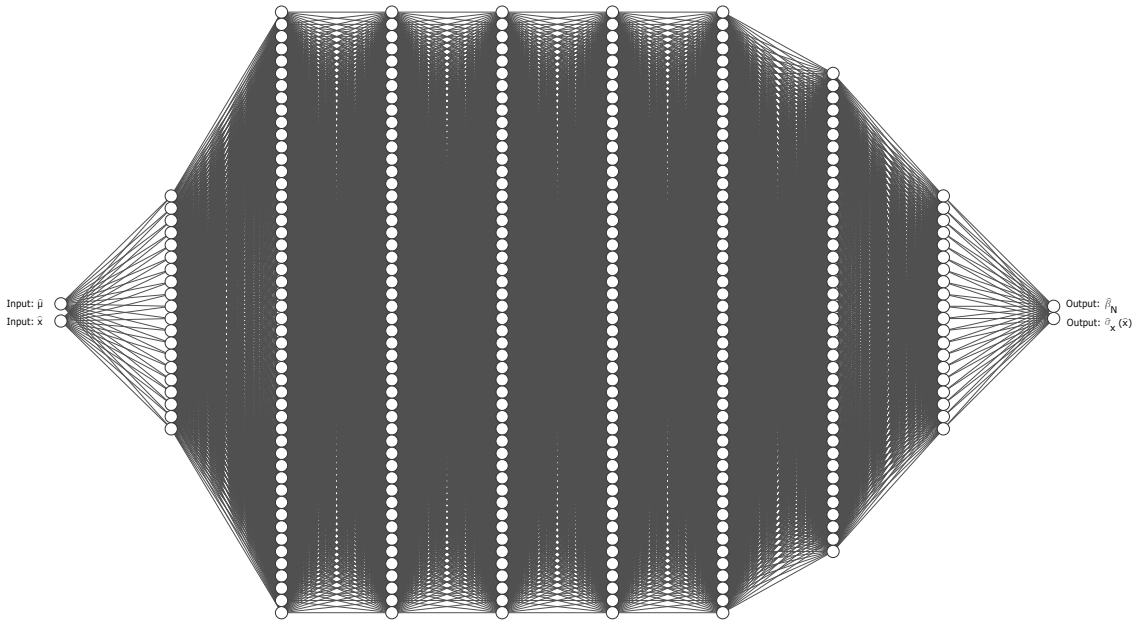

Fig. 2: The forward ANN model for the local stress and neutral point evaluation

For the forward solution of the ODE, we prepare a deep neural network with the input parameters normalized friction coefficient $\hat{\mu}$ and the normalized $\hat{x}$ coordinate. The physical x coordinate, ranging from $x = -l_d$ (entry plane) to $x = 0$ (exit plane) is changed to the normalized $\hat{x}$ so that $\hat{x} = 0$ at entry and $\hat{x} = 1$ at exit by

$$\hat{x} = 1 + \frac{x}{l_d} \Leftrightarrow x = l_d \left(\hat{x} - 1\right). \tag{20}$$

The network's structure is sketched in Figure 2. The first hidden layer has 20 neurons, followed by five hidden layers of 50 neurons each and two more hidden layers of 40 and 20 neurons, finally generating two output features, i.e. the nomalized horizontal stress $\hat{\sigma}_x$ at $\hat{x}$ and the normalized neutral angle β_N. The normalized friction coefficient $\hat{\mu}$ ranges from 0 to 1 according to

$$\hat{\mu} = \frac{\mu - \mu_{min}}{\mu_{max} - \mu_{min}}. \tag{21}$$

The network will predict the normalized horizontal stress $\hat{\sigma}_x$ and the normalized neutral angle $\hat{\alpha}_N$. The network is trained with a set of friction coefficients ranging from μ_{min} to μ_{max}. In contrast to conventional ANN training where target outputs must be supplied, we leverage a custom loss function to assess the alignment of the derivatives of the predicted stresses with the given differential equation. The boundary conditions on the horizontal stresses for given strip tensions t_0 and t_1 are enforced by a suitable normalization of the output stress. We require $\hat{\sigma}_x = \hat{t_0}$ at $\hat{x} = 0$ and $\hat{\sigma}_x = \hat{t_1}$ at $\hat{x} = 1$. We do this by transforming $\hat{\sigma}_x$ to the physical stress σ_x using

$$\sigma_x = C\left(\hat{\sigma}_x - \hat{s}_0 - \hat{s}_1\right) \tag{22}$$

with

$$\hat{s}_0 = \left(\hat{\sigma}_{x0} - \hat{t}_0\right)\left(1 - \hat{x}\right) \tag{23}$$

and

$$\hat{s}_1 = \left(\hat{\sigma}_{x1} - \hat{t}_1\right)\hat{x}. \tag{24}$$

C is a normalizing factor in the order of magnitude of the maximum physical stress, for cold rolling of steel strips, typically $C \approx 1000$. $\hat{\sigma}_{x0}$ and $\hat{\sigma}_{x1}$ are the predicted $\hat{\sigma}_x$ values at roll gap entry and exit,

respectively. The original form of the physical ODE in Equation 1 is now further elaborated to an expression for $d\sigma_x/dx$ and replacing dh/dx by Equation 5,

$$\frac{d\sigma_x}{dx} = \frac{2}{h}\left[\sigma_N - \frac{x}{R}\left(\sigma_x \mp \tau_F\right)\right]. \tag{25}$$

In the loss function, we want to use this ODE in the normalized form $\frac{d\hat{\sigma}_x}{d\hat{x}}$. Differentiating Equation 22 with respect to x, we get

$$\frac{d\sigma_x}{dx} = \frac{C}{l_d}\left(\frac{d\hat{\sigma}_x}{d\hat{x}} - \frac{d\hat{s}_0}{d\hat{x}} - \frac{d\hat{s}_1}{d\hat{x}}\right), \tag{26}$$

from which it follows in combination with Equation 25 that

$$\frac{d\hat{\sigma}_x}{d\hat{x}} = \frac{l_d}{C}\frac{2}{h}\left[\sigma_N - \frac{l_d\left(\hat{x}-1\right)}{R}\left(\sigma_x \mp \tau_F\right)\right] - \left(\hat{\sigma}_{x0} - \hat{t}_0\right) + \left(\hat{\sigma}_{x1} - \hat{t}_1\right). \tag{27}$$

with σ_x from Equation 22. For cold rolling, we define the shear stress τ_F according to slipping friction with $\tau_F = \mu\sigma_N$. As can be seen from the double sign in the preceding equations, τ_F must undergo a sign change at the neutral point. When the boundary conditions are automatically satisfied by the above normalization and satisfaction of the ODE is enforced by the loss minimization, the neutral point is the only unknown. We therefore include the neutral point position as an output parameter to make the network select it appropriately. This output has its own output layer and the sigmoid activation function

$$\sigma\left(x\right) = \frac{1}{1+e^{-x}} \tag{28}$$

is applied to ensure $\hat{\alpha}_N \in [0;1]$. To retain differentiability, no abrupt change of the direction of shear stresses should be introduced. Instead, a smooth transition will be formulated using a tanh approach based on the neutral point position $\hat{x}_n$. Therefore,

$$\tau_F = -\mu\sigma_N \tanh\left[D\left(\hat{x} - \hat{x}_N\right)\right] \tag{29}$$

where D is a scaling parameter for the smoothness of the transition in the order of magnitude of $D \approx 100$. The normal stress σ_N, required several times in the final ODE, is a function of σ_x by the yield criterion and the vertical force decomposition. Firstly, we express the physical relation between σ_x and a vertical stress σ_z by Tresca's yield criterion

$$\sigma_z - \sigma_x = k_f, \tag{30}$$

when compressive stresses are defined as positive values. The relation between σ_z and σ_N is defined from the vertical force decomposition as

$$\sigma_N = \frac{\sigma_z}{1 \mp \mu\tan\alpha}. \tag{31}$$

Finally, the loss is calculated on each training batch using the loss function

$$\mathcal{L} = \left\| G - \frac{d\hat{\sigma}_x}{d\hat{x}} \right\|^2, \tag{32}$$

where G are the gradients of the predicted stress values calculated by automatic differentiation using PyTorch's autograd engine, and $d\hat{\sigma}_x/d\hat{x}$ are the physical gradients given by Equation 27. Note that we do not need to include the satisfaction of the boundary conditions in the loss function as the normalization applied above provides that the network is unable to predict a result which does not satisfy the

boundary conditions. After evaluation of the network, the forward slip resulting from the predicted neutral angle is evaluated based on Equation 19, giving

$$\kappa = \cos\alpha_N \frac{h_1 + 2R\,(1 - \cos\alpha_N)}{h_1} - 1. \tag{33}$$

The network was trained for a cold rolling pass of fixed geometry with an initial strip thickness of h_0 = 1.0 mm, exit strip thickness of h_1 = 0.7 mm at a roll diameter of R = 400 mm. The network was trained with 40 friction coefficients μ ranging from 0.03 and 0.15. The hyperparameters used in the training are learning rate 10^{-5}, batch size 768 at 15000 epochs. This model is referred to as the forward model, as it calculates the neutral point position and resulting forward slip from the given friction coefficient.

Inverse model and determination of friction coefficients. The purpose of the inverse model is to to predict the friction coefficient from a given forward slip. This inversion can be performed easily using the present neural network approach without any further iteration necessary. For this purpose, an inverse PINN is trained, taking the normalized neutral point $\hat{\alpha}_N$ and the normalized coordinate $\hat{x}$ coordinate as input values, yielding the constant normalized friction coefficient $\hat{\mu}$ and the horizontal stress at position x, $\hat{\sigma}$ as outputs. Beforehand, the neutral angle must be calculated from the nonlinear equation Equation 19. Without further simplifications, the solution is

$$\cos\alpha_N = \frac{2\psi \pm \sqrt{4\psi - 8\psi\,(\kappa+1) + 4\psi^2 + 1} + 1}{4\psi}, \tag{34}$$

where

$$\psi = \frac{R}{h_1}. \tag{35}$$

Out of the two mathematical solutions, the second one with the negative double sign can be omitted as it does not provide resonable results. We can however simplify this equation when we disregard one of two $\cos\alpha_N$ expressions from Equation 19 and arrive at

$$cos\alpha_N \approx 1 - \frac{\kappa}{2\psi}. \tag{36}$$

For the inverse training of the network, only a slight change to the loss function is necessary compared to the forward version, i.e. the friction coefficient must be taken from the model predictions and the neutral point from the input parameters.

Results

All calculations are performed for a strip material C15 with the cold flow curve given by $k_f = 850 \cdot \varphi^{0.23}$. Figure 3 shows the horizontal stress distributions predicted by the forward neural network for different friction coefficients, together with stress distributions calculated by numerical solution of von Karman's differential equation, resembled by the dotted lines.

As can be seen from these results, the stress distributions produced by the neural network include the typical sign change in the frictional shear stress at the neural point, leading to a peak value of the horizontal stress. Therefore, it is evident that the model is capable of selecting the neutral point position according to the given coefficient of friction. The inverse model predicts the stress distributions as a function of the given neutral point positions. Figure 4 shows the normal stress distributions for nominal forward slips κ between 0.01 and 0.06. The dotted lines represent the stress distributions, which were recalculated numerically from the friction coefficients predicted by the neural network.

Table 1 shows the results concerning the resulting friction coefficients, along with the predicted normalized neutral point positions. These predicted friction coefficients were then used to recalculate

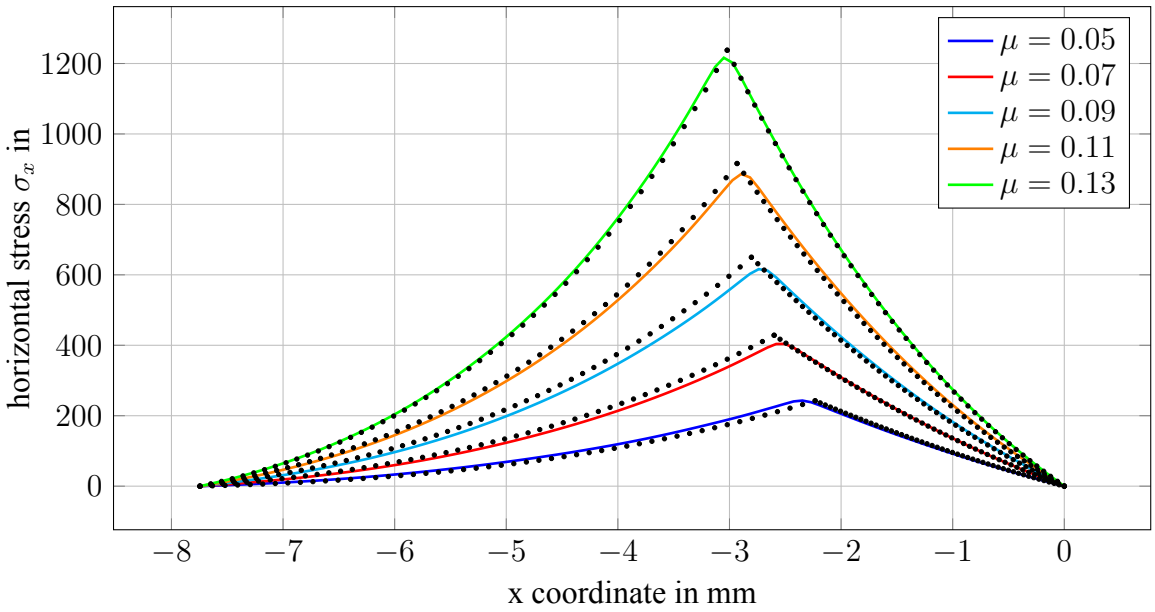

Fig. 3: Horizontal stress distributions predicted by the Forward PINN, compared to results of numerical solution of the ODE (dots)

Table 1: Nominal forward slip values κ, friction coefficients and neutral points predicted by the neural network, and numerically calculated forward slips from the predicted friction coefficients

κ	μ	β_N	κ_{back}
0.01	0.027	0.153	0.009
0.02	0.034	0.216	0.019
0.03	0.045	0.265	0.031
0.04	0.059	0.265	0.042
0.05	0.076	0.265	0.051
0.06	0.092	0.265	0.057

the forward slip values using the direct numerical solution. These back-predictions are shown as κ_{back} in Table 1.

Figure 5 shows the difference between the neural network and numerical model for a continuous range of forward slips at the cold rolling pass under consideration.

Both models predict higher friction coefficients at higher forward slips, though there are differences in the absolute friction coefficients predicted for higher forward slips and friction coefficients. The red dots indicate the numerical results when roll flattening is accounted for by Hitchcock's equation for steel rolls with the Young's modulus E = 210 GPa and the Poisson's coefficient ν = 0.3,

$$\frac{R'}{R} = 1 + \frac{CF_S}{\Delta h}, \tag{37}$$

with the specific roll force per unit strip width F_S, where

$$C = \frac{16}{\pi}\frac{1-\nu^2}{E}. \tag{38}$$

At this stage, it shall be noted that the numerical iterative technique requires the complete stress distributions to be calculted in order to connect the neutral point to the friction coefficient. For the ANN, this is not needed and the evaluation of a single point of this stress-distribution is sufficient to determine the friction coefficient μ associated to a given normalized neutral angle β_N. We will call this technique the *single-point ANN evaluation* in constrast the *full ANN evaluation*; the only difference

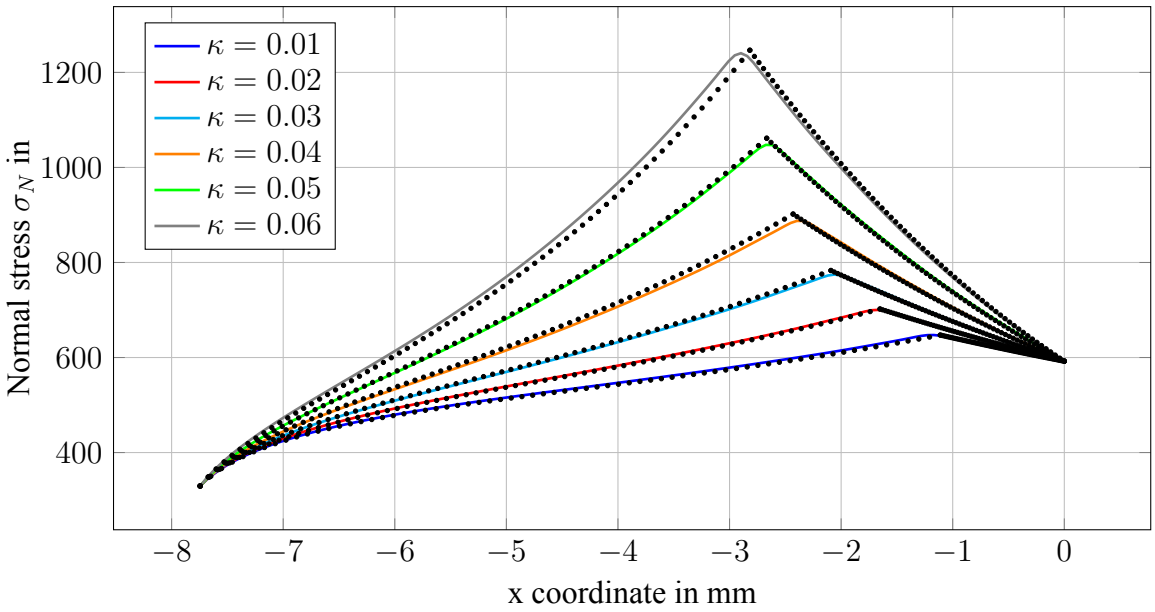

Fig. 4: Normal stress distribution calculated by the inverse network for given forward slips, and the numerically calculated stress distributions for the predicted friction coefficients (dots)

is that the latter technique generates the stress distribution at multiple points as another informative result.

As we expect the single-point evaluation to be faster than the full ANN evaluation, it will be interesting to compare the evaluation times of both inverse ANN in comparison to the inverse classical solution, as the purpose of the present study is to significantly speedup the evaluation by using the ANN. Table 2 shows the evaluation times for the three variants considered (full ANN evaluation with stress distribution $t_{ANN,full}$, single-point ANN evaluation without stress distribution $t_{ANN,sp}$, classical inverse method t_{class}). The mean evaluation times were determined at 1000 equal evaluations of each method.

Table 2: Nominal forward slip values κ, friction coefficients and mean evaluation times

κ	μ_{ANN}	μ_{class}	$t_{ANN,full}$ [ms]	$t_{ANN,sp}$ [ms]	t_{class} [ms]
0.01	0.027	0.028	0.562	0.227	15.18
0.02	0.034	0.035	0.590	0.252	16.08
0.03	0.045	0.044	0.474	0.225	15.89
0.04	0.059	0.056	0.549	0.253	16.64
0.05	0.076	0.074	0.544	0.282	20.58
0.06	0.092	0.104	0.563	0.272	20.49

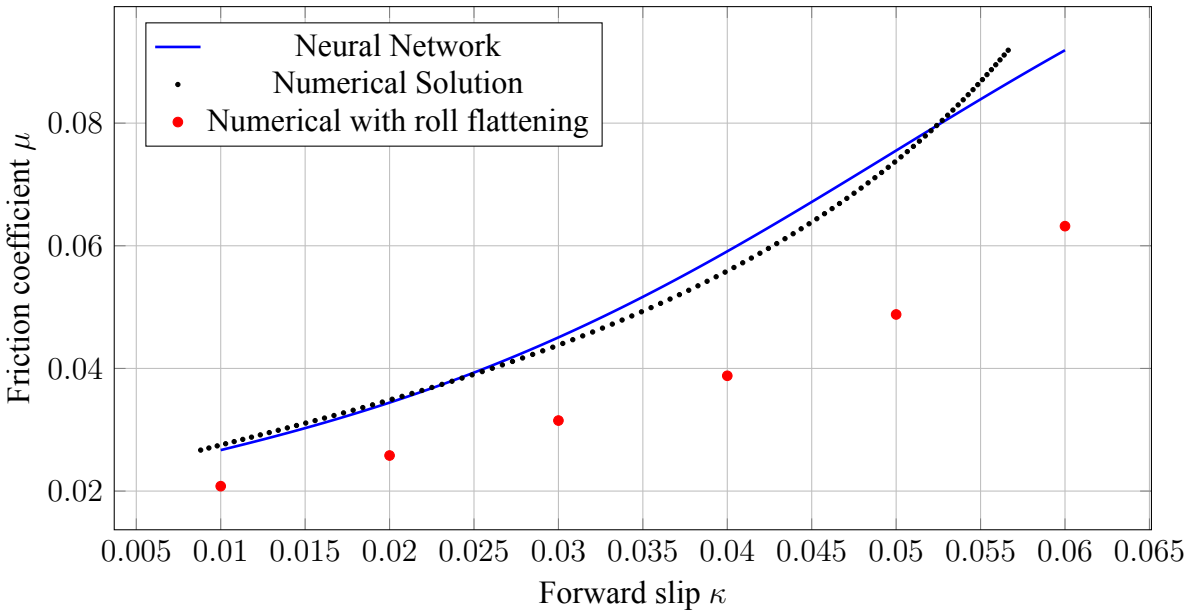

Fig. 5: Relation of friction coefficient and forward slip according to neural network and numerical solution

Discussion

The present contribution demonstrates the construction of a physics-informed neural network which is capable of solving von Karman's ordinary differential equation of the roll gap in cold strip rolling for both forward and inverse analyses of friction in cold rolling. The forward model is capable of selecting the neutral point position according to the given friction coefficient and implement the sign change of the frictional shear stresses accordingly. The inverse model uses a given neutral point position which may be initially calculated from a measured forward slip and selects the friction coefficient so that the final solution satisfies the underlying differential equation, as well as the boundary conditions and the given neutral point. However, if the classical numerical technique is employed to solve this problem, multiple iterations are required to perform an inverse parameter fit for the friction coefficient. This problem is overcome by the present neural network based solution. It should also be noted that it is not necessary to calculate the total stress distribution throughout the roll gap to achieve the connection between forward slip and friction coefficient; the evaluation of the ANN at one single x-value is sufficient, which provides an additional performance boost to the new model. A similar method of calculating the stress distribution in rolling by a PINN is not yet found elsewhere in the literature. The comparison of evaluation times as seen in Table 2 reveals a substantial speedup of the ANN evaluation in comparison to the classical inverse evaluation method. If only the friction coefficient is of interest, the single-point evaluation method can be employed, achieving a calculation which is more than 60 times faster than the classical method. The full ANN evaluation including the local stress distribution is still about 30 times faster than the classical method. In view of this speedup, the additional training time required to set-up the PINN of about 15-20 minutes even for 15000 training epochs is more than justified.

In the current model, elastic roll flattening is not taken into account, an effect prevalent in cold strip rolling, affecting the length of the contact region and stress distribution. However, the inclusion of roll flattening in the model is possible by adding the satisfaction of Hitchcock's equation to the loss function. This extension would only increase the training effort substantially as the roll force must be calculated for each training epoch, but would not affect the evaluation speed, leading to further tremendous increases of the model performance compared to the classical iterative numerical technique. Therefore, it is planned to extend the model to elastic roll flattening and to address this extension in future publications.

References

[1] J. M. Alexander. On the theory of rolling. *Proceedings of the Royal Society of London. Series A, Mathematical and Physical Sciences*, 326(1567):535–563, 1972.

[2] D. Dresden. Ueber das voreilen beim walzen. *Z. angew. Math. Mech.*, 5(1):78–79, 1925.

[3] W. Hessenberg and R. Sims. The Effect of Tension on Torque and Roll Force in Cold Strip Rolling. *Journal of the Iron and Steel Institute*, 168:155–164, 1951.

[4] M. Jarl. Friction and forward slip in hot rolling. *Scandinavian Journal of Metallurgy*, 17(2), 1988.

[5] J. Jeswiet, M. Arentoft, and P. Henningsen. Methods and devices used to measure friction in rolling. *Proceedings of the Institution of Mechanical Engineers, Part B: Journal of Engineering Manufacture*, 220(1):49–57, 2006-01-01.

[6] J. G. Lenard. Friction and forward slip in cold strip rolling. *Tribology Transactions*, 35(3):423–428, 1992-01.

[7] E. Li, A. Tieu, and W. Yuen. Forward slip measurements in cold rolling by laser doppler velocimetry: uncertainty analysis and accuracy improvement. *Journal of Materials Processing Technology*, 133(3):348–352, 2003-02.

[8] S.-E. Lundberg. Evaluation of friction in the hot rolling of steel bars by means of on line forward slip measurements. *Scand J Metallurgy*, 33(3):129–145, 2004-06.

[9] E. Orowan. The calculation of roll pressure in hot and cold flat rolling. *Proceedings of the Institution of Mechanical Engineers*, 150(1):140–167, 1943-06.

[10] C. Overhagen and R. Martin. Roll pass design for round and square sections using an informed artificial neural network. *Materials Research Proceedings*, 44:444–455, 2024-09-15.

[11] A. Paszke, S. Gross, F. Massa, A. Lerer, J. Bradbury, G. Chanan, T. Killeen, Z. Lin, N. Gimelshein, L. Antiga, A. Desmaison, A. Kopf, E. Yang, Z. DeVito, M. Raison, A. Tejani, S. Chilamkurthy, B. Steiner, L. Fang, J. Bai, and S. Chintala. PyTorch: An imperative style, high-performance deep learning library [software].

[12] H. Pawelski. *Interaction between mechanics and tribology for cold rolling of strip with special emphasis on surface evolution*. Technische Universität Bergakademie Freiberg, 2004.

[13] M. Raissi, P. Perdikaris, and G. Karniadakis. Physics-informed neural networks: A deep learning framework for solving forward and inverse problems involving nonlinear partial differential equations. *Journal of Computational Physics*, 378:686–707, 2019-02.

[14] A. M. Roy and S. Guha. A data-driven physics-constrained deep learning computational framework for solving von mises plasticity. *Engineering Applications of Artificial Intelligence*, 122:106049, 2023-06.

[15] E. Siebel and W. Lueg. Untersuchungen über die spannungsverteilung im walzspalt. *Mitteilungen aus dem Kaiser-Wilhelm-Institut fuer Eisenforschung*, 15:1–14, 1933.

[16] C. Smith, F. Scott, and W. Sylwestrowicz. Pressure distribution between stock and rolls in hot and cold flat rolling. *Journal of the Iron and Steel Institute*, 170:347–359, 1952.

[17] G. Van Rooyen and W. Backofen. Friction in cold rolling. *J. Iron Steel Inst.*, pages 235–244, 1957.

[18] R. Venter and A. Abd-Rabbo. Modelling of the rolling process—i. *International Journal of Mechanical Sciences*, 22(2):83–92, 1980-01.

[19] T. von Karman. Beitrag zur theorie des walzvorgangs. *Z. angew. Math. Mech.*, 5(2):139–141, 1925.